On the preparation of TiO_2-sepiolite hybrid materials for the photocatalytic degradation of TCE: influence of TiO_2 distribution in the mineralization

Silvia Suárez[a], Juan M. Coronado[a], Raquel Portela[a] Juan Carlos Martín[b], Malcolm Yates[b] Pedro Avila[b], Benigno Sánchez[a]

a) CIEMAT, PSA, Aplicaciones Ambientales de la Radiación Solar

Avda. Complutense nº 22, Building 42, 28040 Madrid, Spain,

Tel.: +34 91 346 61 77, FAX: +34 91 346 60 37, e-mail: silvia.suarez@ciemat.es

b) Instituto de Catálisis y Petrolequímica, CSIC. C/ Marie Curie nº 2, 28049 Madrid, Spain

Abstract

Hybrid structured photocatalysts based on sepiolite, an adsorbent, and TiO_2 were prepared by extrusion of ceramic dough and conformed as plates. The influence of the photocatalyst configuration was studied either by including TiO_2 in the extrusion process (incorporated materials) or by coating the sepiolite plates with a TiO_2 film (coated materials). The influence of the OH^- surface concentration in the photocatalytic performance was studied by treating the ceramic plates at different temperatures. The samples were characterized by N_2 adsorption-desorption, MIP PIM, SEM, XRD, UV-vis-NIR spectroscopy and tested in the photocatalytic degradation of trichloroethylene (TCE) as a target VOC molecule. Most of the catalysts presented high photoactivity but considerable differences were observed when the CO_2 selectivity was analyzed. The results demonstrate that there is a significant effect of the catalyst configuration on the selectivity of the process. An intimate contact between the sepiolite fibers and TiO_2 particles for incorporated materials with a corncob-like structure favored the migration of non desiderable reaction products such as $COCl_2$ and dichloroacetylchloride (DCAC) to the adsorbent, reacting with OH^- groups of the adsorbent and favoring the TCE mimeralization.

Introduction

Photocatalysis is an efficient, attractive and clean technology for pollutant abatement either in aqueous media or in gas phase (*1*). The photocatalytic process is adequate for the treatment of low flow of effluents with low concentration of contaminants. TiO_2 is the archetypal photocatalytic material since it is endowed with a high inherent photocatalytic activity (*2*). Moreover, within the industrial sector the usage of TiO_2 particles is not feasible due to the high cost of the concomitant filtration facilities needed to recover the catalyst. For this reason, supported photocatalysts are required.

An attractive alternative consists in the development of *conformed hybrid photocatalytic materials,* which by combining adsorption and photocatalytic properties induce a synergism towards abatement of pollutants (*3, 4*). These systems may attenuate the variation in the concentration of pollutant agents, maintaining good photocatalytic efficiency. The overall abatement process will be of dual nature, based on the physisorption of pollutants on the adsorbent material followed by their rapid diffusion towards the photocatalytic-adsorption centers interface. Thus, silica beds (*5*), pillared clays (*6*), ceramic membranes (*7*), mesoporous material (*8*) zeolites (*9*) and activated carbon (*10*) have been studied. Sepiolite is a light and inexpensive material used as an adsorbent due to its high surface area and porosity (*11*). This clay is extensively used as cat litters, for waste treatment (removal of pesticides), moisture control and animal feedstuffs (additive E-562). According to Bellman et al. the sepiolite from Tolsa S.A (Madrid, Spain), presents a low biological activity due to the short length of its fibers (*12*). Moreover it is used as catalytic support due to the improvement in the mechanical strengths of TiO_2 and Al_2O_3 based catalysts (*13*).

The role of sepiolite in the catalytic process is not totally clear. In fact, it has been suggested that this silicate may play a role in the migration of oxygen species and hydrogen spillover (*13*) (*14*). In the case of a photocatalytic process the diffusion of OH radicals on illuminated TiO_2 has been reported from different studies. Tatsuma *et al.* observed a remote oxidation of organic dyes separated from a TiO_2-coated plate by a small gap (*15*). Remote photodegradation of self-assembled monolayers of aliphatic chains anchored to an inert silicon surface confirmed the diffusion action of oxidizing species on the TiO_2 surface (*16*). Lee and Choi (*17*) demonstrated that the OH radicals generated on the TiO_2 surface migrated beyond 80 μm to mediate the oxidation of carbon soot. Nevertheless, to our knowledge no studies have been reported about the role of sepiolite on the migration of intermediates specie during a photocatalytic process.

In the present work we have studied the photocatalytic performance of hybrid materials in a plate structure, similar to conventional borosilicate plates, considering important parameters for scale up such as low cost of the preparation method and easy manipulation of the photocatalysts. The role of sepiolite in the photocatalytic process was studied analyzing the effect of TiO_2 and sepiolite particles distribution and OH^- surface groups in the photocatalytic activity and selectivity using trichloroethylene (TCE) as a model molecule.

Experimental Section

Preparation of SiMgOx plates

Magnesium silicate (Tolsa S.A) was used to prepare the ceramic plates. The composition of the magnesium silicate, expressed as oxides, was SiO_2: 59,50%, MgO:17,55 %, Al_2O_3:6,26%, CaO: 2.36 wt.%, Fe_2O_3: 1.84 wt.%, Na_2O: 0.53 wt.%, K_2O: 1.73 wt.%. The powder samples were mixed and kneaded with water until ceramic dough with the optimal plasticity was obtained (*18*). The plates were obtained by extrusion using a specifically designed die. The fresh samples were dried at room temperature for seven days, then at 110ºC for 24 hours and finally heat treated at 500ºC or 800ºC for 4 hours. The resulting plates presented the following dimensions: 9.0 x 2.8 x 0.3 mm (length x width x thickness).

Preparation of SiMgOx-TiO_2 incorporated plates

Commercial TiO_2 (G-5 Millenium) were mixed with sepiolite using the same procedure described above. The TiO_2 purity was higher than 98 % with a sulfate content between 0.8-1.7 wt.%, P_2O_5 <0.4 wt.% and Na_2O and K_2O < 0.01 wt.%. After heat treatment the sepiolite:TiO_2 ratio by weight was 1:1.

Preparation of SiMgOx-TiO_2 covered plates

A water dispersion of TiO_2 G-5 (30 g/l) acidified with nitric acid 1 M was prepared by ultrasonic treatment during 30 min. The $SiMgO_x$ plates treated at different temperatures were immersed in the TiO_2 suspension at a constant rate (3 $mm \cdot s^{-1}$). The samples were dried at 100ºC after the coating. This process was repeated four times in order to ensure the total coverage of the surface. The materials were finally heat treated at 500ºC for 4 h. For comparative purposes a borosilicate glass plate was prepared by a dip coating technique starting from a TiO_2 sol (*19).*

The ceramic plates were denominates as *$SiMgOx_a/TiO_2$-b* where “a” indicate the temperature treatment of the support and “b” refers to the preparation method, (-i) for incorporated and (-c) for covered materials (Table 1).

Catalysts characterization

The specific surface area (S_{BET}) of the samples was calculated from *nitrogen adsorption at* 77 K determined with a Carlo Erba Sorptomatic 1800. The pore volumes were analyzed by use of *Mercury Intrusion Porosimetry* (MIP) using CE Instruments Pascal 140/240 porosimeter, after drying the samples at 423 K overnight. The total pore volumes

were determined by combination of nitrogen adsorption (0-50 nm) and mercury intrusion porosimetry (50-300 μm) results. *X-ray diffraction* (XRD) patterns of ground samples were recorded on a Phillips PW1710 powder diffractometer using CuKα radiation: λ = 0.154 nm. *UV-Vis absorption* spectra of the plates were collected with a LAMBDA 950 UV-Vis-NIR spectrophotometer between 2,500-300 nm wavelength with 10 nm step.

The scanning electron microscopy and energy dispersive X-ray spectroscopy studies were performed in a Zeiss DSM 960 Digital Scanning Microscope, coupled with an analyzer of dispersive energies EXD Link eXL. Samples were coated with a conductive layer of graphite to minimize charging effects.

Photocatalytic activity test

The photocatalytic oxidation of trichlotoethylene (TCE) was studied in a continuous plug flow gas-phase flat photoreactor. The photoreactor with external dimensions 120 x 50 x10 mm (length x wide x thickness) was made of stainless steel except for one face where a window of 30 cm^2, made of pyrex glass, was placed for photocatalyst illumination provided by two UVA Philips TL-8W/05 fluorescent lamps with a maximum emission at 365 nm wavelength and light intensity 4.4 $mW \cdot cm^{-2}$. A gas mixture of TCE and air was prepared using gas cylinder of TCE/N_2 (Air Liquide, 500 ppm) and compressed air free of water and CO_2. The flow rate was controlled by using electronic mass flow controllers. The TCE concentration was varied between 10-200 ppm, and the total gas flow from 240 to 700 $ml \cdot min^{-1}$. The gas composition was monitored continuously using a FTIR Thermo-Nicolet 5700 spectrometer, provided with a temperature controller multiple reflection gas cell (optical path 2 m) maintained a 110ºC.

Results and discussion

The textural properties of the raw materials and sepiolite base materials treated at different temperatures are collected in Table 1. It should be noticed that the coated materials with a TiO_2 content around 0.9 wt.% had similar textural properties as SiMgOx plates alone. The materials treated at 350ºC displayed poor mechanical strength that made them unsuitable for practical applications. Nevertheless, the characterization data are included for comparative purposes.

Catalysts characterization

The TiO_2 particles morphology and distribution on covered and incorporated materials was studied by *Scanning Electron Microscopy* (Figure 1). Natural magnesium silicate presents a fibrous structure ranging from 0.2 to 2 μm in length and 0.1 to 0.3 μm in diameter for the bundles of fibers (*20*). The space in-between the bundle of fibers provides the material with the porosity essential for the TiO_2 adhesion. The micrograph depicted in Figure 1a for coated material, reveals that TiO_2 is deposited as a homogenous film on the SiMgOx. A certain number of cracks can be detected probably as a result of tension forces generated by the solvent evaporation during the drying and heat treatment process. Only sphere shaped particles due to TiO_2 aggregates covering the surface were observed. The statistical analysis of 200 particles in $SiMgOx_{800ºC}/TiO_2$-c gave a Gaussian distribution with a maximum around 200 nm and with 80% of particles with size between 120-320 nm. XEDS line profile analyses of coated plates prepared with different numbers of layers indicated that four layers were the optimum to successfully cover the surface with a layer thickness of around 10 μm. In Figure 1b SEM micrograph of the incorporated material treated at 500ºC is shown. The fibrous structure of the magnesium silicate can be appreciated but covered with TiO_2 particles of around 20 nm (corresponding to the primary particle size of commercial TiO_2) forming a corncob-like structure, increasing the bundle size. For sample treated at 800ºC areas enriched in TiO_2 were easy to find indicating that higher temperature treatment favors the TiO_2 sintering and reduces the dispersion on the silicate fibers.

The textural properties of raw materials and samples based on sepiolite treated at different temperatures are presented in Table 1. The magnesium silicate powders had a specific surface area of 148 $m^2\ g^{-1}$ (250 ºC). The extrusion process hardly modified the surface area of the materials treated at similar temperature. The raw material presented a mesoporous structure associated with the interparticulate packing, the contribution from micropores being negligible. Sample treated up to 500ºC showed a bimodal pore size

distribution with maximum at 14 nm and 28 nm (see Figure S1 Supporting Information). With higher pretreatment temperatures the material sintered, causing a loss in specific surface area and a shift in the intraparticulate porosity to wider pores with a maximum at 35 nm. The incorporation of TiO_2 leads to a shifting of the pore diameter from 28 nm to 44 nm ascribed to the separation between bundles due to adhesion of TiO_2 to the bundles of fibers**.** Heat treatment at 800ºC resulted in a shift of pore size from 14 nm to 28 nm and from 28 to 55 nm as a consequence of both the modification of the silicate structure and TiO_2 sintering.

TiO_2 G-5 presents TiO_2-anatase as the only crystalline phase (ASTM 21-1272) even at 800ºC. The incorporated materials prepared with TiO_2 and SiMgOx maintain the same TiO_2 crystalline phase detected for TiO_2 G-5 and the characteristic diffraction peaks of sepiolite (ASTM 26-1226) (see Figure S2 Supporting Information). The average crystal size was estimated using Scherrer's equation (Table 1). The crystal size ranges from 7.7 nm for the fresh sample to 46.7 nm for TiO_2-G5 treated at 800ºC. The mixture of TiO_2 with the SiMgOx impedes the growth of TiO_2 crystals by sintering process favored at high temperature. When these two components were mixed and kneaded during the extrusion process, an intimate contact between the fibrous structure of the silicate and the TiO_2 particles was established avoiding TiO_2 agglomeration, in agreement with SEM study.

In order to know the nature of the OH groups, incorporated materials treated at different temperatures were analyzed by UV-Vis-NIR DRS (**Figure 2).** For comparison sepiolite plates were also analyzed (Figure S3 Supporting Information). The intensity of the bands centered at 1,400 nm, 1,910 nm and 2,300 nm decreased as the heat treatment temperature was increased. The spectra is characteristic of a water rich material showing an intense absorption band at 1,900 nm due to the combination of the H-O-H bending and O-H stretching modes (*21*). Less pronounced absorption peaks also appear at 1,400 nm and 2,300 nm. The band at 1,400 nm is the typical first overtone of the O-H stretch. Moreover the band at 2,300 nm is the combination of Mg-OH bending, O-H stretching combination and Al-OH bend in minor proportion. The incorporation of TiO_2 produced a strong decrease of the reflectance in the UV region at 300 nm corresponding to titania absorption of light. At 800ºC the band at 2300 nm practically disappeared probably because the presence of TiO_2 favored the lost of the OH surface groups associated to Mg. Two features explain the decreasing of the intensity of the OH associated bands after the incorporation of TiO_2. The total amount of silicate was halved after incorporation of TiO_2 but more importantly, free OH groups were the anchoring sites for the bonding of TiO_2 to the silicate particles.

Photocatalytic activity results

In order to analyze the role of the hydroxyl groups belonging to the support the experiments were performed without water vapor in the gas feed. The temperature inside the photocatalytic reactor at the steady state conditions was 35ºC. At this temperature, no photolytic reaction was observed and neither an important effect in the photocatalytic process is expected (*22*)**.** A strong effect of the pretreatment temperature on the catalytic performance for incorporated materials was observed. Thus, conversions above 80 % were achieved for *$SiMgO_{x500ºC}/TiO_2$-i* meanwhile values below 50% were obtained for the material treated at 800ºC. Several effects could justify the decrease of the photocatalytic activity for the plate treated at high temperature: the reduction of the surface area and TiO_2 dispersion with the presence of TiO_2 crystals of larger size as well as the decrease of the concentration of OH^- groups available to carry out the reaction in accordance with the UV-Vis-NIR spectra.

The effect of the total flow in the catalytic performance was also analyzed for coated materials and compared to $SiMgO_{x500ºC}/TiO_2$-i at a higher TCE concentration. As expected, high gas flow produced a decrease in the catalytic activity (**Figure 3.a**). Considering the catalytic activity results the following series was found: $SiMgO_{x800ºC}$ /TiO_2-c > $SiMgO_{x500ºC}/TiO_2$-*i* > *$SiMgO_{x500ºC}/TiO_2$ -c*. Taking into account that the coated materials have the same TiO_2 loadings, the difference observed was related to the catalysts porosity and TiO_2 distribution on the surface. The support treated a 500ºC presented higher porosity and TiO_2 was mainly inside the porous structure of the support, not accessible to the photons of the UV radiation.

The major reaction products detected in the outlet were CO_2, $COCl_2$, DCAC and small amounts of CO, HCl were also found (*23*). The CO_2 selectivity data are represented in **Figure 3a**. The selectivity of the incorporated material treated at 500ºC was higher than 40 % showing the highest CO_2 values and the lower signal of $COCl_2$ (Figure 3.b). It is well known that OH radicals initiate the TCE photocatalytic reaction according to Eq.1. In our case the experiments were conducted without water and reaction takes place with the OH^- surface groups provided by the hybrid material. The formation of $COCl_2$ and DCAC was explained by Eq. 2 and Eq.3 and considering consecutive reactions pathways. High residence time favored $COCl_2$ meanwhile DCAC was suppressed, suggesting that DCAC was able to continue the reaction to produce $COCl_2$ (Ec. 3); On the contrary at low residence times the reaction stopped at the first step (Ec. 2) (*24*).

$$C_2HCl_3 + 2O_2 + H_2O \rightarrow 2CO_2 + 3HCl \quad \text{Eq. 1}$$

$$C_2HCl_3 + 1/2O_2 \rightarrow C_2HCl_3O \quad \text{Eq. 2}$$

$$C_2HCl_3O + 1/2O_2 \rightarrow COCl_2 + HCl + CO_2 \quad \text{Eq. 3}$$

The dependence of the TCE conversion with the TCE partial pressure was studied, using a total gas flow of 700 ml/min and TCE concentration between 10-200 ppm (**Figure 4**). Borosilicate glass coated by five layers of TiO_2 prepared by the sol gel method was tested in similar conditions of residence time; although a formal comparison is not possible because of the obvious differences in the preparation method, TiO_2 particle size, titania loading and nature of support some considerations can be pointed out.

In the case of the borosilicate glass plate there is an exponential decay of the photoactivity and CO_2 selectivity with TCE concentration, and only 30% TCE conversion was achieved with 70 ppm of TCE in the inlet. Above 50 ppm of TCE the $COCl_2$ strongly increased along with a decrease of the DCAC intensity (Figure 4.b); the low quantity of TCE reacted mainly to produce $COCl_2$.

The shape of the curves was different for hybrid photocatalysts because of the adsorption component and the TiO_2 loading. The catalytic activity curves showed the same tendency observed previously, where the incorporated material kept a good photocatalytic activity and the highest CO_2 selectivity. A typical behavior of a Langmuir-Hinshelwood mechanism where the reactants are molecularly adsorbed was observed (*25*) (see Figure S4 Supporting Information). The reaction rate increased with the TCE concentration up to 100 ppm where it was kept constant, except for the incorporated material. At TCE concentrations higher than 100 ppm the active sites were saturated with TCE and thus, an increase in the TCE concentration did not produce any modification in the reaction rate. For the incorporated material a constant value was not achieved due to the higher TiO_2 loading that requires a higher concentration of TCE to saturate the surface. Higher TCE concentration resulted in higher DCAC (Figure 4.b), CO and HCl signals (not shown). $COCl_2$ curves presented a maximum dependent on the catalysts configuration and coincident with the point in which the reaction rate reached a maximum and consequently the TCE conversion curves slope changed.

The inspection of $COCl_2$ and DCAC curves revealed an opposite trend compared to the borosilicate glass plate. These results pointed out the important role of the support in the reaction selectivity. In the case of the borosilicate glass, the lifetime of DCAC on the surface

was very short due to the low adsorption capacity and DCAC was not able to react to produce $COCl_2$; only at high concentration of TCE the reaction goes on to produce $COCl_2$. Nevertheless, the high adsorption capacity of hybrid materials leads to longer lifetime of intermediate species and then DCAC may react to produce $COCl_2$ at low TCE concentration.

The catalysts configuration is a crucial factor in the selectivity according to Blake et al. (*24*). Comparing catalysts with different geometries the authors concluded that the non photocatalytic hydrolysis reaction of $COCl_2$ takes places in the dark interior of alumina pellets. These results support the hypothesis of the key role that magnesium silicate plays in $SiMgOx_{500ºC}/TiO_2$-m, as a source of the OH^- surface groups, keeping the TiO_2 active sites free from reaction intermediates due to the intimate contact between titania and magnesium silicate. Thus, these properties resulted in an improvement of the CO_2 selectivity compared to coated materials where the migration of intermediate species was less favored.

Different phenomena have to be considered to optimize the photocatalytic performance: the porosity of the support that may affect the quantity of TiO_2 exposed to the photons in coated materials, the presence of OH^- groups necessary to carry out the photocatalytic process and the distance between the TiO_2 actives sites and OH groups. A schematic diagram of the dual function observed in incorporated materials is presented in Scheme 1: sepiolite acts as a buffer of TCE due to its adsorbent properties, keeping constant TCE concentration in the vicinity of TiO_2 active sites (a), and the corncob-like structure allow the diffusion of non desiderable reaction products with the subsequent reaction with OH^- groups of the sepiolite, improving the TCE mineralization (b). Thus, the incorporated material treated at 500ºC presented an acceptable photocatalytic activity and the highest selectivity to CO_2 compared to coated materials. The hybrid materials developed in this study present a simple, quick and cheap method to prepare supported photocatalysts, that may minimize possible variation in the gas feed composition and avoid the expensive filtration processes required for catalysts recuperation.

Acknowledgement

The authors are grateful to the Spanish Science and Innovation Ministry, CTQ2004-08232-C02-01 / PPQProject and Juan de la Cierva Program, for financial support.

Supporting information

Figure S1. Total pore volume and pore distribution for sepiolite plates treated at different temperatures.
Figure S2. XRD diffractograms for *SiMgOx/TiO_2-i* and commercial TiO_2 G-5 with temperature.
Figure S3. UV-Vis spectra of magnesium silicate plates treated at different temperatures.

Figure S4. Reaction rate variation with TCE concentration.

This information is available free of charge via the Internet at http://pubs.acs.org.

BRIEF

The hybrid TiO_2-sepiolite photocatalyst allows to modify photoactivity and selectivity towards CO_2, acting as adsorbent and source of OH^- groups.

TABLES

Table 1. Textural properties of TiO_2 powder samples, coated and incorporated ceramic plates at different temperatures with TiO_2 crystal size

Materials	T[a] treatment, °C	BET area $m^2\ g^{-1}$	Meso-	Macro-	Crystal size nm
			pore volume, $cm^3\ g^{-1}$		
TiO_2 (sol-gel)	350	158	0.25	-	3.9
TiO_2	250	321	0.23	-	7.7
SiMgOx	250	148	0.33	-	-
$SiMgOx_{350°C}/TiO_2$-c	350	141	0.34	0.18	-
$SiMgOx_{500°C}/TiO_2$-c	500	126	0.32	0.24	-
$SiMgOx_{800°C}/TiO_2$-c	800	68	0.25	0.27	-
$SiMgOx_{350°C}/TiO_2$-i	350	175	0.40	0.20	7.2
$SiMgOx_{500°C}/TiO_2$-i	500	153	0.40	0.22	10.9
$SiMgOx_{800°C}/TiO_2$-i	800	63	0.29	0.23	23.9

Figures

Figure 1. Scanning electron micrographs of a) covered and b) incorporated materials.

a) **b)**

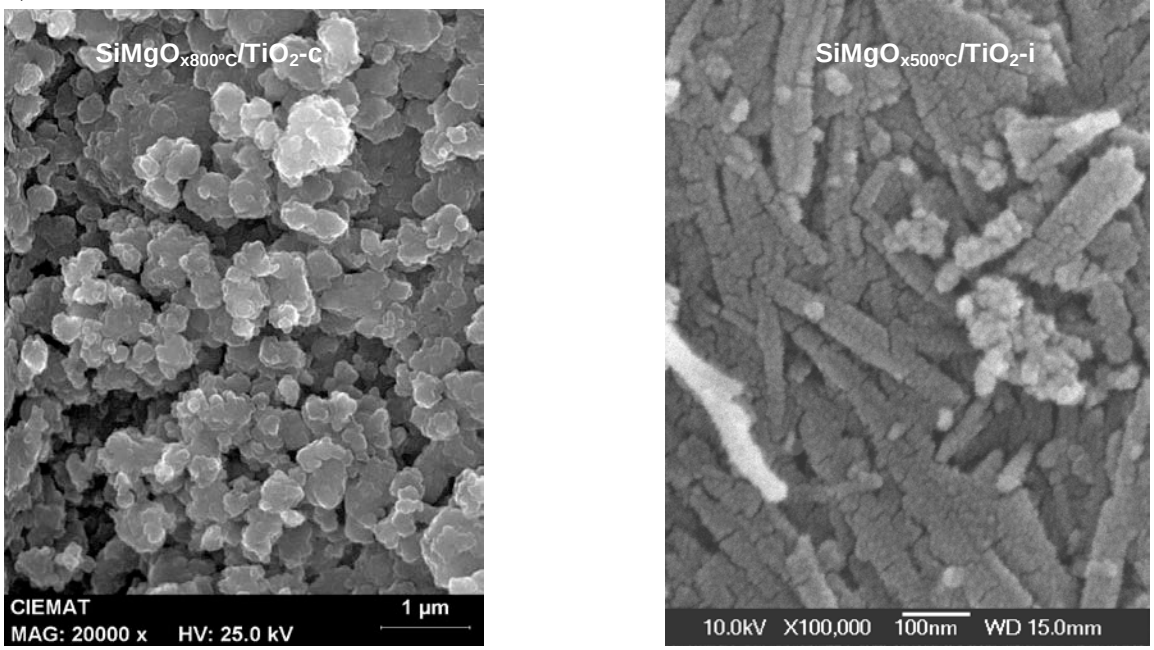

Figure 2. UV-Vis spectra for *SiMgOx/TiO$_2$-i* materials treated at different temperatures.

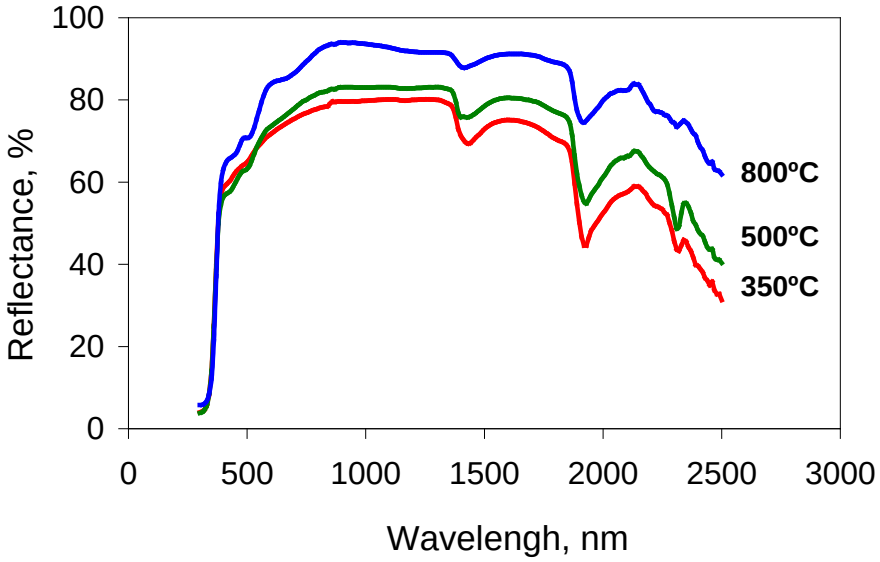

Figure 3. a) TCE conversion (filled figures) and CO_2 selectivity (empty figures) and b) $COCl_2$ (filled figures) and DCAC signals (empty figures) with total flow referred to the illuminated area for catalysts: (▲,△) *SiMgO$_{x800}$/TiO$_2$-c* (■, □) *SiMgOx$_{500}$/TiO$_2$-c* (●,○) *SiMgOx$_{500}$/TiO$_2$-i*. Gas feed composition: [TCE]= 90 ppm, balance = air. Operating conditions: flow= 300-700 ml min^{-1}, GHSV = 3,500-8,000 h^{-1}, t_r= 1.0-0.4 s, v_L= 0.2-0.5 cm s^{-1}.

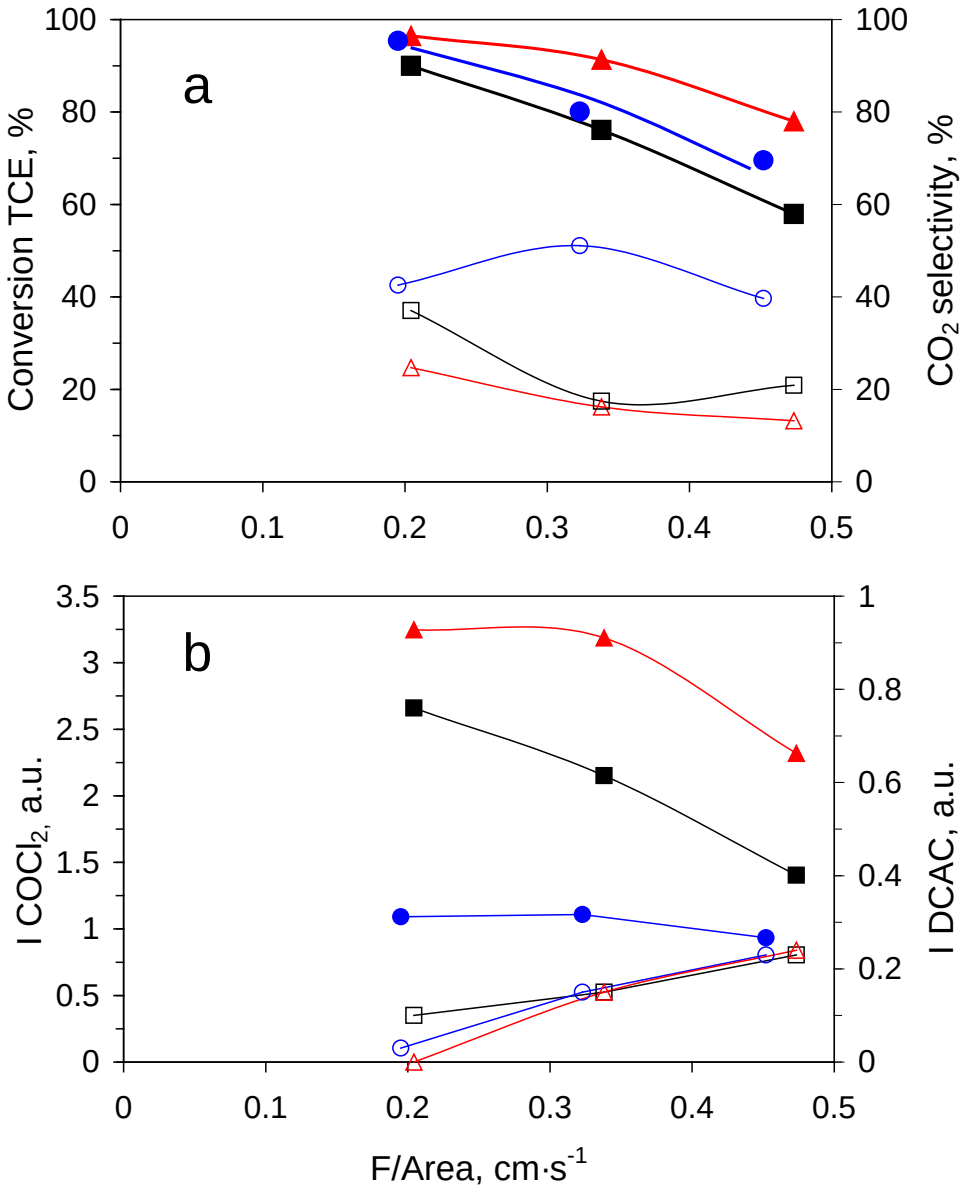

Figure 4. a) Variation of the TCE conversion (filled figures) and CO_2 selectivity (empty figures) and b) $COCl_2$ (filled figures) and DCAC (empty figures) signals with TCE concentration for (▲,△) $SiMgO_{x800}/TiO_2$-c (■,□) $SiMgOx_{500}/TiO_2$-c (●,○) $SiMgOx_{500}/TiO_2$-i (♦,◇) glass plate/TiO_2 sol. Operating conditions: flow= 700 ml min^{-1}, GHSV= 8,500 h^{-1}, t_r= 0.4 s, v_L= 0.5 cm s^{-1}. Operating conditions for glass plate experiment: GHSV = 5,000 h^{-1}, t_r= 0.72 s, v_L= 0.3 cm s^{-1}

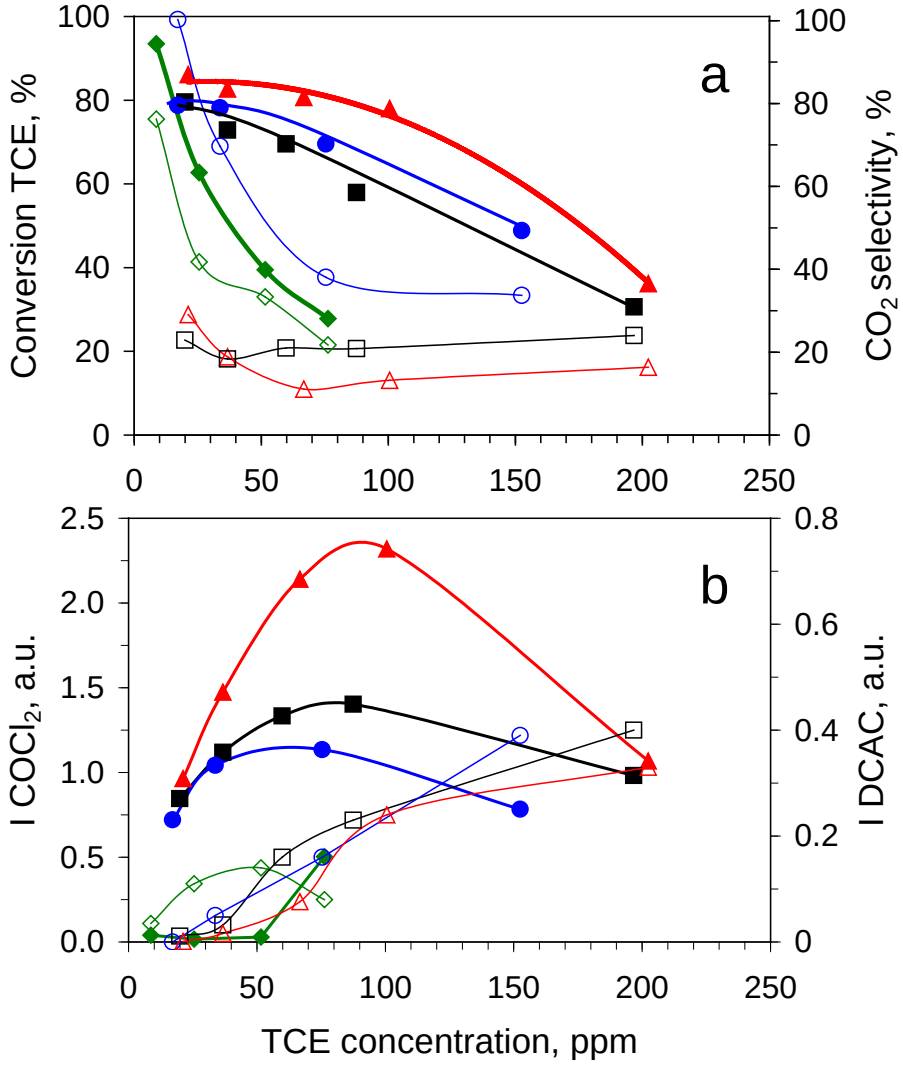

Scheme 1. Dual function of a TiO_2-sepiolite hybrid photocatalysts: a) adsorption of TCE and b) adsorption-reaction with OH^- groups of non desirable reaction products (○) TiO_2 particles and (▭) sepiolite bundle of fibers.

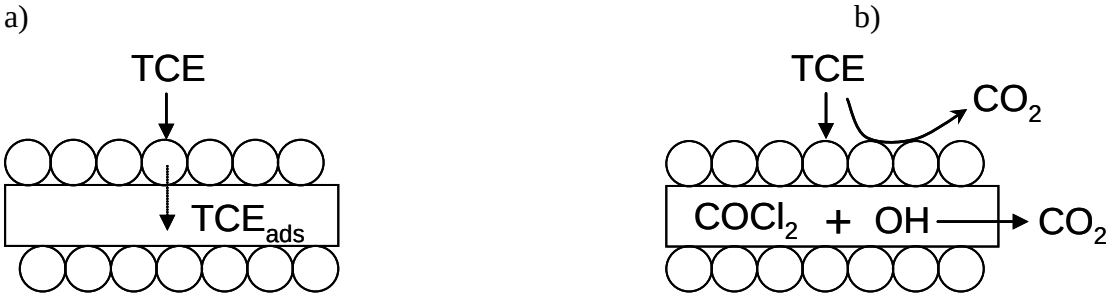

Literature Cited

(1) Fox M. A., Dulay M., Heterogeneous. Photocatalysis *Chem. Rev.* 1993, 9*3*, 341-357.

(2) Carp O., Huisman C.L., Reller A., Photoinduced reactivity of titanium dioxide, Prog. Solid State Ch. 2004, 32, 33-177.

(3) Takeda N., Torimoto T., Sampath S., Kuwabata S., Yoneyama H., Effect of inert for titanium dioxide loading on enhancement of photodecomposition rate of gaseous propionaldehyde, J. Phys. Chem. 1995, 99 (24), 9986-9991.

(4) Legrini O., Oliveros E., Braun A., Photochemical Processes for Water Treatment, Chem. Rev. 1993, 93 (2), 671-698.

(5) Mohseni M., Gas Phase Trichloroethylene (TCE) Photooxidation and Byproduct Formation: Photolysis vs. Titania/Silica based Photocatalysis, Chemosphere 59 (2005) 335-342.

(6) Ooka C., Yoshida H., Suzuki K., Hattori T., Effect of surface hydrophobicity of TiO_2-pillared clay on adsorption and photocatalysis of gaseous molecules in air, Appl. Catal. A, 2004, 260 (1), 47-53.

(7) Kwak S-Y., Kim S.H., Hybrid Organic/Inorganic Reverse Osmosis (RO) Membrane for Bactericidal Anti-Fouling. 1. Preparation and Characterization of TiO_2 Nanoparticle Self-Assembled Aromatic Polyamide Thin-Film-Composite (TFC) Membrane, Environ. Sci. Technol. 2001, 35 (11), 2388-2394.

(8) Wittman G., Demeestere K., Dombi A., Dewulf J., Van Langenhove H., Preparation, structural characterization and photocatalytic activity of mesoporous Ti-silicates, Appl. Catal. B 2005, 61 (1-2) 47-57.

(9) Ichiura H., Kitaoka T., Tanaka H., Removal of indoor pollutants under UV irradiation by a composite TiO_2–zeolite sheet prepared using a papermaking technique, Chemosphere, 2003, 50 (1), 79-83.

(10) Torimoto T., Ito S., Kuwabata S., Yoneyama H., Effects of Adsorbents Used as Supports for Titanium Dioxide Loading on Photocatalytic Degradation of Propyzamide, Environ. Sci. Technol. 1996, 30, 1275-1281.

(11) Alvarez A., Sepiolite: properties and uses. Pp. 253-289 in Palygorskite-Sepiolite. Occurrences, genesis and Uses (A. Singer and E. Galán, Editors). Developments in Sedimentology, Nr. 37, Elsevier, Amsterdam, 1984.

(12) Bellman B., Muhle H., Ernst H. Investigations on heatlht-related properties of two sepiolite samples, Environmental Health Perspectives 1997, 105 (5) 1049-1052.

(13) Suárez S., Yates M., Petre A.L., Martín J.A., Avila P., Blanco J., Development of a new Rh/TiO_2-sepiolite monolithic catalsyts for N_2O decomposition, Appl. Catal. B 2006, 64 (3-4) 302-311.

(14) Baeza P., Villarroel M., Avila P., Agudo A.L., Delmon B., Gil-llambias F.J., Spillover hydrogen mobility during Co–Mo catalyzed HDS in industrial-like conditions, Appl. Catal. A 2006, 304, 109-115.

(15) Tatsuma T., Tachibana S., Miwa T., Tryck D.A., Fujishima A., Remote Bleaching of Methylene Blue by UV-Irradiated TiO_2 in the Gas Phase, J. Phys. Chem B. 1999 103 (38), 8033-8035.

(16) Haick, H., Paz, Remote Photocatalytic Activity as Probed by Measuring the Degradation of Self-Assembled Monolayers Anchored near Microdomains of Titanium Dioxide, Y. J. Phys. Chem. B 2001, 105 (15), 3045-3051.

(17) Lee, M.C., Choi, W., Solid Phase Photocatalytic Reaction on the $Soot/TiO_2$ Interface: The Role of Migrating OH Radicals, J. Phys. Chem. B 2002, 106 (45), 11818-11822.

(18) J. Blanco, A. Romero, EP patent 0978313A1 (2000).

(19) Sánchez B., Coronado J.M., Candal R., Portela R., Tejedor I., Anderson M., Tompkins D., Lee T., Preparation of TiO_2 coatings on PET monoliths for the photocatalytic elimination of trichloroethylene in the gas phase, *Appl. Catal. B* 2006, *66 (3-4), 295-301*.

(20) S. Suárez, C. Saiz, M. Yates, J.A. Martin, P. Avila, J. Blanco, $Rh/\gamma\text{-}Al_2O_3$–sepiolite monolithic catalysts for decomposition of N_2O traces, Appl. Catal. B 2005, 55 (1) 57-64.

(21) Clark R.N., King T.V.V., Klejwa M., Swayze G., Vergo N., High spectral resolution reflectance spectroscopy of minerals, J. Geophys. Res. 1990, 95 (B8) 12653-12680.

(22) Sanchez B., Cardona A.I., M. Romero, Avila P, Bahamonde A., Influence of temperature on gas-phase photo-assisted mineralization of TCE using tubular and monolithic catalysts, Catal. Today 1999, 54 (2-3) 369-377.

(23) Driessen M.D., A.L. Goodman, Miller T.M., G.A. Zaharias, Grassian V.H., Gas-Phase Photooxidation of Trichloroethylene on TiO_2 and ZnO: Influence of Trichloroethylene Pressure, Oxygen Pressure, and the Photocatalyst Surface on the Product Distribution, J. Phys. Chem. 1998, 102, 549-556.

(24) Jacoby W.A, Nimlos A.R.,. Blake D.M, “Products, intermediates, mass balances, and reaction pathways for the oxidation of TCE in air via heterogeneous photocatalysis” Environ. Sci. Technol. 1994, 28 (9) 1661-1668.
(25) Jacoby W.A, Blake D.M, Noble R.D., Koval C.A. “Kinetics of the Oxidation of Trichloroethylene in Air via Heterogeneous Photocatalysis” J. Catal. 1995, 157, 87-96.

On the preparation of TiO_2-sepiolite hybrid materials for the photocatalytic degradation of TCE: influence of TiO_2 distribution in the mineralization

Silvia Suárez[a], Juan M. Coronado[a], Raquel Portela[a] Juan Carlos Martín[b], Malcolm Yates[b] Pedro Avila[b], Benigno Sánchez[a]

a) CIEMAT, PSA, Aplicaciones Ambientales de la Radiación Solar

Avda. Complutense nº 22, Building 42, 28040 Madrid, Spain,

Tel.: +34 91 346 61 77, FAX: +34 91 346 60 37, e-mail: silvia.suarez@ciemat.es

b) Instituto de Catálisis y Petrolequímica, CSIC. C/ Marie Curie nº 2, 28049 Madrid, Spain

Figure S1. a) Total cumulative pore volume and b) pore volume distribution curves obtained by N_2 adsorption and MIP of magnesium silicate plates treated at (◇) 350ºC, (○) 500ºC, (□) 800ºC.

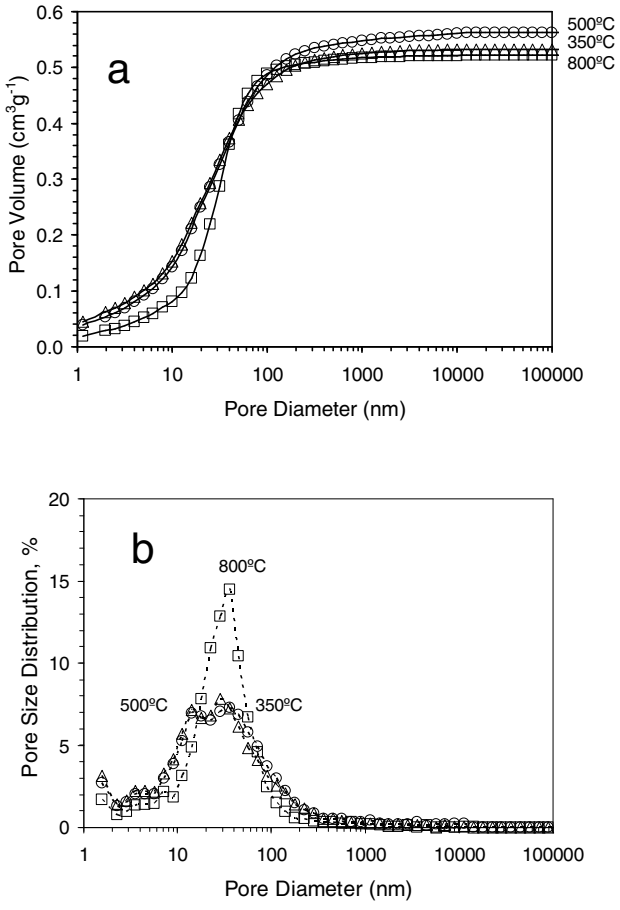

Figure S2. XRD diffractograms for *SiMgOx/TiO$_2$-i* and commercial TiO$_2$ G-5 treated at different temperatures: (○)TiO$_2$-anatase (□) TiO$_2$-rutile (◇) sepiolite.

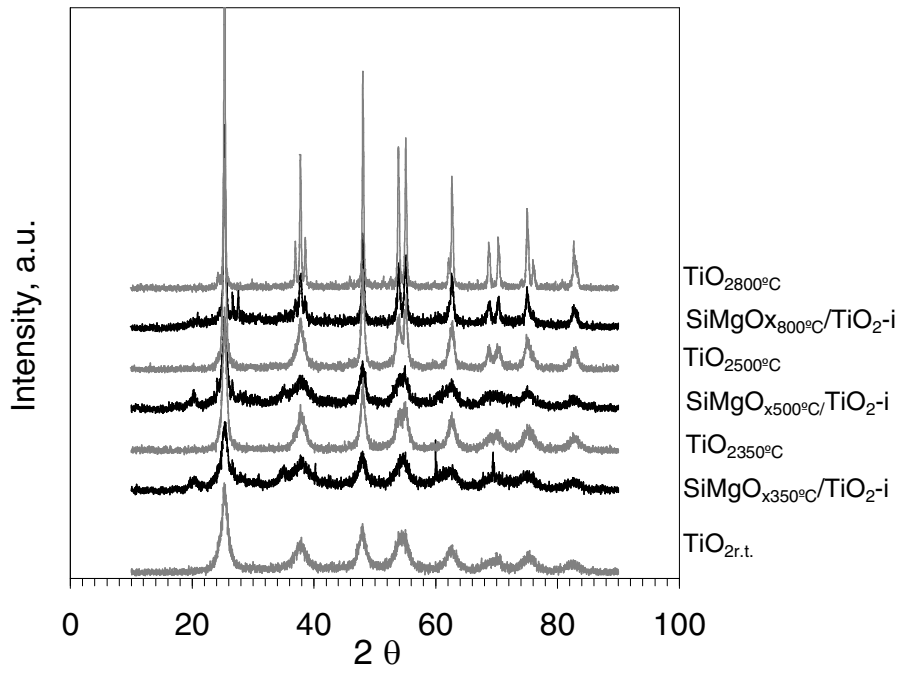

Figure S3. UV-Vis spectra of magnesium silicate plates treated at different temperatures.

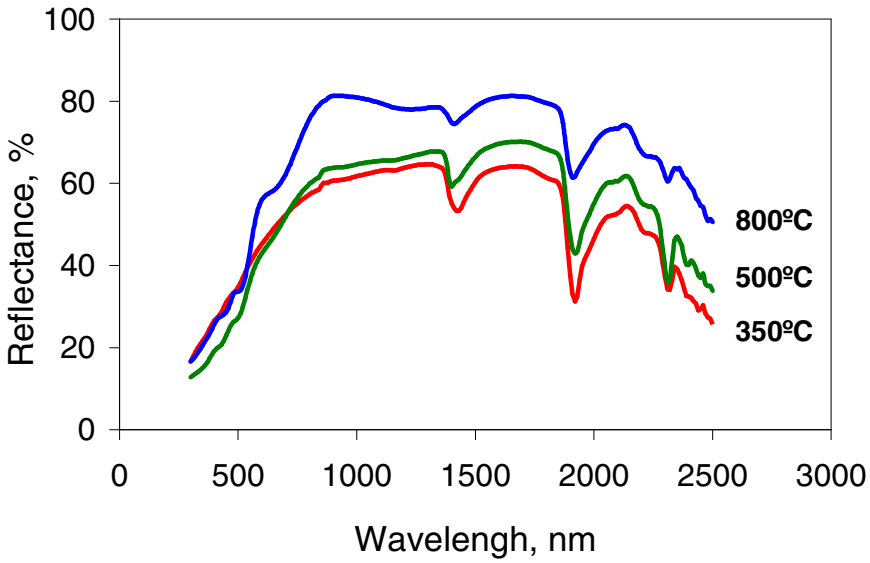

Figure S4. Reaction rate variation with TCE concentration in the gas inlet for: (▲) $SiMgO_{x800}/TiO_2$-c , (■) $SiMgOx_{500}/TiO_2$-c, (●)$SiMgOx_{500}/TiO_2$-i.